July, 1981] © *1981 The Chemical Society of Japan* *Bull. Chem. Soc. Jpn.*, **54**, *2183—2188 (1981)* 2183

The Fluidity and Electrolytic Conductivity of Alkali-metal Chloride/Poly(ethylene oxide)-H_2O Systems. The Effects of the Polymer Concentration and the Temperature

Toshiaki Isono,* Katsuo Takahashi, and Reita Tamamushi

The Institute of Physical and Chemical Research, 2-1 Hirosawa, Wako, Saitama 351

(Received December 17, 1980)

The fluidities of poly(ethylene oxide) (PEO)–H_2O mixtures and the electrolytic conductivities of alkali-metal chlorides in the PEO–H_2O mixtures were measured at different PEO compositions and temperatures (25—50 °C). The extended Walden's rule was found to be satisfied when the fluidity and conductivity were changed by the temperature variation at a constant composition, whereas a large deviation from Walden's rule was observed upon the isothermal variation of the PEO composition. The Arrhenius activation parameters were determined from the temperature dependence of the fluidities and conductivities, and some correlations between pairs of parameters were examined.

The mobility of ions and molecules in solution generally decreases with a decrease in the fluidity of the solution; the simplest relationship between the ionic mobility and fluidity is given by the well-known Stokes law (or Walden's rule);

$$\lambda^{\infty}/\phi = \text{const}, \tag{1}$$

where λ^{∞} is the limiting ionic conductivity, and ϕ, the fluidity of the solution. In viscous solutions containing large polymer molecules, however, the mobility of small particles has been known to show significant deviations from Walden's rule;[1] but it can be approximately represented by the empirical equation;[2–4]

$$\lambda^{\infty}\phi^{-p} = \text{const}, \tag{2}$$

where $0<p<1$.

Different theoretical approaches, such as the concepts of "microscopic viscosity" and "obstruction effect," have attempted to interpret the influence of large neutral molecules on the mass-transport properties of small ions and molecules.[2,5] From the experimental point of view, it seems important to find empirical correlations between pairs of various physical quantities concerning the mass-transport process; although the physical meaning of some of these correlations may be difficult to understand, they may be expected to provide useful information for the theoretical study of the structure of solutions and the mechanism of mass-transport phenomena.

In the present work, we have measured the fluidities of aqueous solutions containing poly(ethylene oxide)s (PEO) with relative molecular masses of 200—20000 and the electrolytic conductivities of alkali-metal chlorides (MX) in PEO–H_2O mixtures at different polymer concentrations and temperatures. This PEO series was chosen for the following reasons: (i) pure samples of sufficiently low conductivities are available; (ii) aqueous solutions of a wide range of fluidity can be prepared, and (iii) PEO is a material of practical importance, being very much used for surfactants, detergents, drugs, and polymer solvents in chemical reactions. The Arrhenius activation parameters have been determined from the temperature dependence of the fluidity and conductivity, and some phenomenological correlations between pairs of these parameters will be discussed.

Experimental

Materials. The poly(ethylene oxide)s used were Polyethylene Glycols (PEG 200, PEG 4000, and PEG 20000) as supplied by Wako Pure Chemical Industries, Ltd. The average relative molecular masses of these polymers, as determined by the vapor-pressure method, were 200 for PEG 200, 3300 for PEG 4000, and 11700 for PEG 20000.

The samples of alkali-metal chlorides were special-reagent-grade chemicals and were used without further purification.

All solutions were prepared gravimetrically by using redistilled water. In this paper, the composition of the PEO–H_2O mixture is given in terms of the mass fraction of PEO, and the PEO–H_2O mixture is regarded as the solvent of the MX/PEO–H_2O system.

Fluidity and Conductivity Measurements. The PEO–H_2O mixtures used in this work were assumed to be Newtonian fluids, because a preliminary study using a rotational viscometer showed an approximate proportionality between the shearing stress and the velocity gradient.

Cannon-Fenske and Ubbelohde viscometers were used to measure the fluidity of the solutions of $\phi>5\ \mathrm{Pa^{-1}\,s^{-1}}$ (aqueous solutions of PEG 200 and PEG 4000, and those of PEG 20000 at lower concentrations). Capillary diameters were chosen to give flow times of 60 seconds at least. The fluidities of highly viscous mixtures (aqueous solutions of PEG 20000 at higher concentrations) were measured by means of a falling-ball viscometer consisting of a glass cylindrical tube (inner diameter, 17 mm) and a stainless steel ball (diameter, 1 mm) used in ball bearings. Weld pycnometers were employed to determine the densities of the solutions.

The electrolytic conductivities of 0.1 mol kg^{-1} MX/PEO–H_2O systems were measured by the four-electrode a.c. method that has been described in a previous paper;[6] the electrodes were Pt-wires (diameter, 0.5 mm), and the frequency was 125 Hz, no frequency effect being observed in the range of 60 Hz—1 kHz. This method has definite advantages over the conventional two-electrode method when applied to highly viscous mixtures. The conductivities of the PEO–H_2O mixtures were always less than 1% of those due to the electrolytes and so could be neglected in the calculation of the molar conductivities of MX.

All measurements were made in a constant-temperature water bath which was capable of a controlled temperature of better than $T\ \pm0.05$ K. The accuracy of the measurements was estimated to be better than ±1% for the molar conductivity, ±0.1% for $\phi>5\ \mathrm{Pa^{-1}\,s^{-1}}$, and ±1% for $\phi<1\ \mathrm{Pa^{-1}\,s^{-1}}$; no correction of ϕ was made for the kinetic energy term.

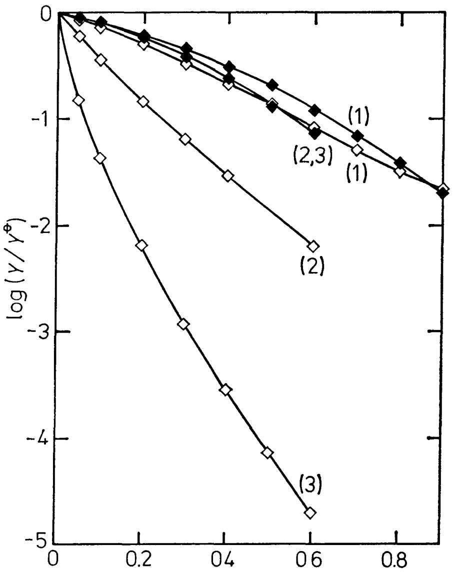

Fig. 1. Changes in the fluidity ($Y=\phi$, —◇—) and the molar conductivity of 0.1 mol kg^{-1} NaCl ($Y=\Lambda$, —◆—) in the PEO–H_2O mixtures at 25 °C as a function of the mass fraction of PEO: (1) PEG 200, (2) PEG 4000, and (3) PEG 20000. Y° represents the fluidity of pure water in the case of $Y=\phi$, and the molar conductivity of 0.1 mol kg^{-1} NaCl in H_2O in the case of $Y=\Lambda$, respectively.

Further details of the experimental procedures and the full experimental data obtained in this work have been reported in a separate paper.[7)]

Results and Discussion

Effect of the Polymer Concentration on the Fluidity and Conductivity. The fluidity of a PEO–H_2O mixture and the molar conductivity of MX in the 0.1 mol kg^{-1} MX/PEO–H_2O system are functions of the polymer concentration and the temperature:

$$Y = Y(w,T) \quad ; \quad Y \equiv \phi \text{ and } \Lambda_{MX}, \tag{3}$$

where the symbol Y represents the fluidity (ϕ) and the molar conductivity of MX (Λ_{MX}), w is the mass fraction of PEO, and T is the absolute temperature. The fluidity and conductivity changes produced by the isothermal variation in the polymer concentration are different in nature from those produced by the temperature variation at a constant composition; this difference should be considered when the relationship between the fluidity and conductivity is to be analyzed.[2)]

Figure 1 shows the fluidity and conductivity changes in 0.1 mol kg^{-1} NaCl/PEO–H_2O systems at 25 °C as a function of the mass fraction of PEO, w; both the fluidity and conductivity decrease with the increase in w. The change in ϕ with the mass fraction, w, was more pronounced with PEO's of larger relative molecular masses, while the change in Λ_{NaCl} was very much less than that of ϕ and was almost independent of the relative molecular mass of PEO. A similar tendency in the fluidity and conductivity changes with the solution composition has also been known in colloidal solutions (sols and/or gels) including large neutral molecules such as gelatin and agar-agar.[1,2)]

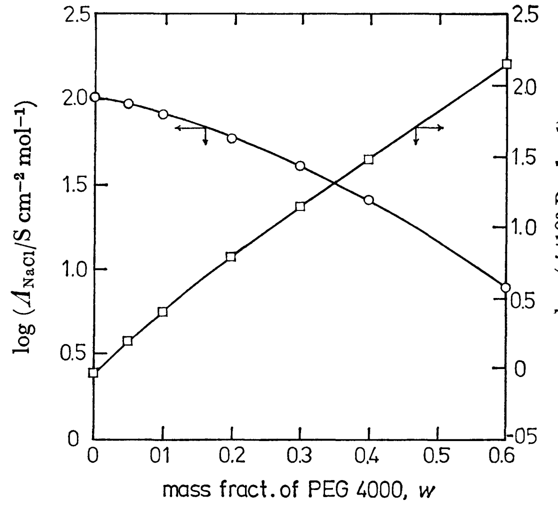

Fig. 2. Composition dependence of the fluidity of PEG 4000–H_2O mixtures and that of the molar conductivity of 0.1 mol kg^{-1} NaCl in PEG 4000–H_2O mixtures (temperature 25 °C): □ and ○ are experimental points; the best-fit equations (4) determined by the least-squares method are shown by solid lines.

Empirically, the isothermal variation in ϕ and Λ_{MX} of the MX/PEO–H_2O system with the mass fraction of PEO can be approximately represented by the equation:

$$\log Y = \sum_{i=0}^{n} a_{i,Y} w^i \quad ; \quad Y \equiv \phi \text{ and } \Lambda_{MX}. \tag{4}$$

In most cases, sufficient accuracy was obtained with $n=3$ for the fluidity of the systems containing PEG 200 and 4000, $n=4$ for the fluidity of the PEG 20000 systems, and $n=2$ for the conductivity. Examples of fitting experimental points by the use of Eq. 4 are given in Fig. 2, where the solid lines represent the empirical equations determined by the method of least-squares.

Temperature Dependence of the Fluidity and Conductivity. The temperature dependence of the fluidities and conductivities of aqueous electrolyte solutions may be represented by an empirical expression of the Arrhenius-type:[8,9)]

$$Y = A_Y \exp(-E_Y/RT) \quad ; \quad Y \equiv \phi \text{ and } \Lambda_{MX}, \tag{5}$$

where E_Y and A_Y are the Arrhenius activation energy and the pre-exponential frequency factor respectively for the viscous flow ($Y\equiv\phi$) and the conductivity ($Y\equiv\Lambda_{MX}$). Over a wide range of temperatures, the Arrhenius plot (ln Y *vs.* T^{-1} plot) for the fluidity of aqueous solutions has been known to deviate from linearity,[10)] which suggests that the activation parameters (E_Y and A_Y) are temperature-dependent or that the Arrhenius-type expression is inadequate. Within a limited range of temperatures, however, the Arrhenius plot generally gives a reasonably straight line and the activation parameters may be regarded as constant.

Some typical Arrhenius plots for the conductivity of the MX/PEO–H_2O systems are shown in Fig. 3, the plots being almost linear over the temperature

Table 1. Activation energies, E_ϕ, and pre-exponential factors, A_ϕ, for the viscous flow of the PEO-H_2O mixtures
(± represents the standard deviation)

System	Mass fraction of PEO	E_ϕ / kJ mol^{-1}	$R \ln (A_\phi/10^3\ \mathrm{Pa^{-1}\ s^{-1}})$ / J mol^{-1} K^{-1}
PEG 200-H_2O	0.05	16.5±0.2	55.0±0.6
	0.1	17.4±0.2	56.7±0.7
	0.2	19.3±0.2	59.8±0.6
	0.3	20.2±0.3	59.7±0.9
	0.4	22.8±0.3	64.6±0.9
	0.5	25.4±0.3	69.4±1.1
	0.6	28.2±0.4	75.0±1.2
	1.0	33.9±0.6	81.6±1.8
PEG 4000-H_2O	0.05	17.3±0.1	54.6±0.5
	0.1	18.9±0.1	56.0±0.4
	0.2	21.2±0.1	56.1±0.4
	0.3	22.6±0.3	53.9±0.8
	0.4	24.8±0.2	54.8±0.7
	0.6	32.6±0.5	68.3±1.5
PEG 20000-H_2O	0.05	21.4±0.2	56.8±0.5
	0.1	21.6±0.1	47.1±0.4
	0.2	20.5±0.1	27.9±0.3
	0.3	21.9±0.2	18.4±0.7
	0.4	23.9±0.2	13.3±0.7
	0.5	27.6±0.4	14.5±1.3
	0.6	33.1±0.5	21.8±1.7

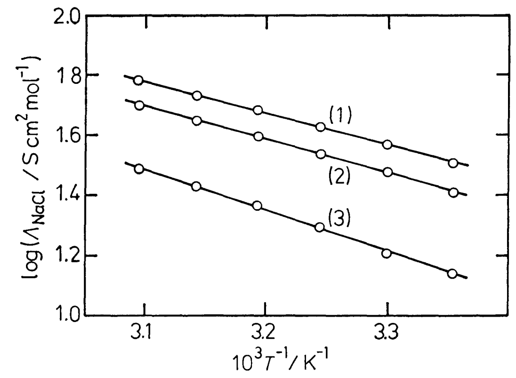

Fig. 3. Arrhenius plots for the molar conductivity of 0.1 mol kg^{-1} NaCl in PEO-H_2O mixtures: (1) PEG 200, w=0.4; (2) PEG 4000, w=0.4; and (3) PEG 20000, w=0.5.

range of 25—50 °C. Similar Arrhenius plots were also obtained for the fluidity of PEO-H_2O mixtures. Tables 1 and 2 present the activation parameters determined from the Arrhenius plots by using the method of least-squares.

Relationship between the Fluidity and Conductivity. The change in the fluidity and conductivity due to the variation of the polymer concentration and temperature can be obtained from Eq. 3 as:

$$dY = \left(\frac{\partial Y}{\partial w}\right)_T dw + \left(\frac{\partial Y}{\partial T}\right)_w dT \tag{6}$$

or:

$$d \ln Y = \left(\frac{\partial \ln Y}{\partial w}\right)_T dw - \frac{1}{T^2}\left(\frac{\partial \ln Y}{\partial T^{-1}}\right)_w dT. \tag{7}$$

Table 2. Activation energies, E_Λ, and pre-exponential factors, A_Λ, for the molar conductivities of 0.1 mol kg^{-1} MX in PEO-H_2O mixtures
(± represents the standard deviation)

System	Mass fraction of PEO	E_Λ / kJ mol^{-1}	$R \ln (A_\Lambda/\mathrm{S\ cm^2\ mol^{-1}})$ / J mol^{-1} K^{-1}
NaCl/PEG 200-H_2O	0.05	14.9±0.1	88±0.4
	0.1	15.5±0.1	89±0.3
	0.2	16.7±0.2	91±1
	0.3	18.4±0.3	94±1
	0.4	20.5±0.3	98±1
	0.5	23.0±0.4	102±1
	0.6	27.1±0.5	112±2
	1.0	30.3±0.9	101±3
KCl/PEG 200-H_2O	0.5	23.6±0.4	105±1
	0.6	27.5±0.5	113±2
NaCl/PEG 4000-H_2O	0.1	15.4±0.1	88±0.3
	0.2	16.7±0.3	90±1
	0.3	18.9±0.2	94±1
	0.4	21.5±0.4	99±1
	0.6	30.1±0.5	118±2
LiCl/PEG 20000-H_2O	0.3	19.0±0.3	93±1
	0.4	21.7±0.4	98±1
	0.5	25.3±0.5	106±2
	0.6	28.9±0.6	113±2
NaCl/PEG 20000-H_2O	0.05	14.7±0.2	87±1
	0.1	15.3±0.3	88±1
	0.2	16.8±0.2	90±1
	0.3	18.9±0.2	94±1
	0.4	21.8±0.4	100±1
	0.5	26.1±0.6	110±2
	0.6	29.8±0.5	117±2
KCl/PEG 20000-H_2O	0.3	19.3±0.2	96±1
	0.4	22.7±0.3	103±1
	0.5	26.9±0.6	112±2
	0.6	30.9±0.5	120±2
RbCl/PEG 20000-H_2O	0.3	19.1±0.3	96±1
	0.4	22.5±0.3	103±1
	0.5	26.9±0.5	112±2
	0.6	30.7±0.4	119±1
CsCl/PEG 20000-H_2O	0.3	18.9±0.2	95±1
	0.4	22.4±0.4	102±1
	0.5	26.9±0.5	112±2
	0.6	30.6±0.6	119±2

The first term on the right-hand side of Eq. 6 or 7 represents the effect of the polymer concentration on the viscous flow and conductivity at a constant temperature, whereas the second term represents the temperature effect at a constant composition.

Using the empirical equations 4 and 5, we can obtain the following expressions:

$$\left(\frac{\partial \ln Y}{\partial w}\right)_T = 2.303 \sum_{i=1}^{n} i a_{i,Y} w^{i-1} \tag{8}$$

and:

$$\left(\frac{\partial \ln Y}{\partial T^{-1}}\right)_w = -\frac{E_Y}{R}, \tag{9}$$

where n=3 or 4 for the fluidity and n=2 for the conductivity.

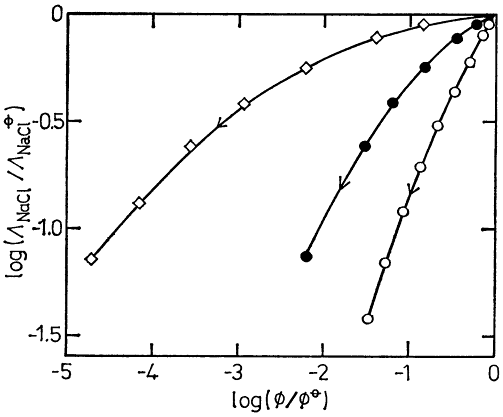

Fig. 4. Plots of $\log(\Lambda_{\mathrm{NaCl}}/\Lambda^{\circ}_{\mathrm{NaCl}})$ against $\log(\phi/\phi^{\circ})$ by the composition variation at 25 °C, where $\Lambda^{\circ}_{\mathrm{NaCl}}$ and ϕ° are the values at $w=0$: —○— PEG 200, —●— PEG 4000, and —◇— PEG 20000. Arrows indicate the direction of increasing PEO-concentration.

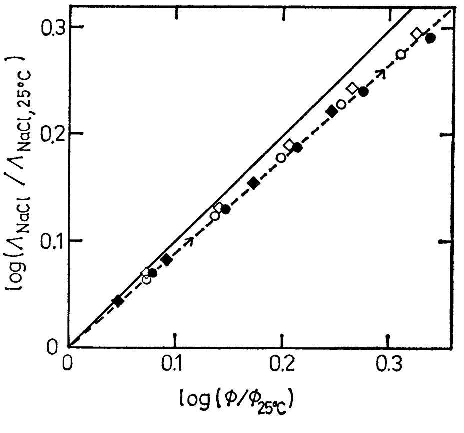

Fig. 5. Plots of $\log(\Lambda_{\mathrm{NaCl}}/\Lambda_{\mathrm{NaCl,25\,^{\circ}C}})$ against $\log(\phi/\phi_{25\,^{\circ}\mathrm{C}})$ by the temperature variation at constant composition, where $\Lambda_{\mathrm{NaCl,25\,^{\circ}C}}$ and $\phi_{25\,^{\circ}\mathrm{C}}$ are the values at 25 °C: —◆— H_2O; —○— PEG 200, $w=0.4$; —●— PEG 4000, $w=0.4$; and —◇— PEG 20000, $w=0.4$. The straight line corresponds to the classical Walden's rule ($p=1$) and the broken line to the extended Walden's rule with $p=0.89$. Arrows indicate the direction of increasing temperature.

From Eqs. 7 and 8, the isothermal change in $\ln\Lambda_{\mathrm{MX}}$ with respect to $\ln\phi$ can be given by:

$$\left(\frac{\mathrm{d}\ln\Lambda_{\mathrm{MX}}}{\mathrm{d}\ln\phi}\right)_T=\left(\frac{\partial\ln\Lambda_{\mathrm{MX}}}{\partial w}\right)_T\Big/\left(\frac{\partial\ln\phi}{\partial w}\right)_T$$
$$=\frac{a_{1,\Lambda}+2a_{2,\Lambda}w}{a_{1,\phi}+2a_{2,\phi}w+3a_{3,\phi}w^2+4a_{4,\phi}w^3}. \qquad (10)$$

This result suggests that, when the concentration of PEO is changed at a constant temperature, the plot of $\ln\Lambda_{\mathrm{MX}}$ against $\ln\phi$ does not give a straight line; in other words, the relation between Λ_{MX} and ϕ deviates from the extended Walden's rule as represented by Eq. 2. Only at sufficiently low concentrations of PEO ($w\ll 1$), the right-hand side of Eq. 10 can be approximated by $a_{1,\Lambda}/a_{1,\phi}$, and the extended Walden's rule may be satisfied.

Similarly, from Eqs. 7 and 9, when the temperature is varied at a constant composition, the change in $\ln\Lambda_{\mathrm{MX}}$ with respect to $\ln\phi$ is given by:

$$\left(\frac{\mathrm{d}\ln\Lambda_{\mathrm{MX}}}{\mathrm{d}\ln\phi}\right)_w=\left(\frac{\partial\ln\Lambda_{\mathrm{MX}}}{\partial T^{-1}}\right)_w\Big/\left(\frac{\partial\ln\phi}{\partial T^{-1}}\right)_w=\frac{E_\Lambda}{E_\phi}. \qquad (11)$$

Since the activation energies, E_Λ and E_ϕ, are nearly independent of the temperature, the $\ln\Lambda_{\mathrm{MX}}$ *vs.* $\ln\phi$ plot by the temperature variation is expected to be linear in accordance with the extended Walden's rule. A comparison of Eqs. 2 and 11 gives the following expression for the p coefficient:

$$p=E_\Lambda/E_\phi. \qquad (12)$$

The experimental data are consistent with the above-mentioned consideration. Some examples of the relation between $\log\Lambda_{\mathrm{NaCl}}$ and $\log\phi$ upon the isothermal variation in the PEO composition are given in Fig. 4. Upon the variation in the temperature at a constant composition, however, $\log\Lambda_{\mathrm{NaCl}}$ changes linearly with $\log\phi$, as is shown in Fig. 5.

Correlations between Pairs of Activation Parameters. The values of the p coefficient as determined from the $\log\Lambda_{\mathrm{MX}}$ *vs.* $\log\phi$ plots were nearly independent of the composition of the MX/PEO–H_2O system, the average value being 0.89±0.07. Because of the relationship given by Eq. 12, this result is equivalent to the existence of a linear correlation between E_Λ and E_ϕ, as is shown in Fig. 6. In this figure, the broken line represents the relation, $E_\Lambda/E_\phi=0.89$ while the solid line corresponds to the best-fit equation:

$$E_\Lambda=(0.97\pm0.04)E_\phi-(2.52\pm0.92)\,\mathrm{kJ\,mol^{-1}}, \qquad (13)$$

where ± represents the standard deviation. The relatively large standard deviations for these two lines suggest that the difference between them can not be regarded as very significant.

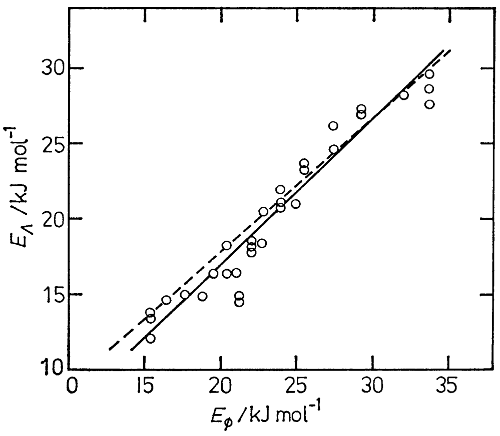

Fig. 6. Correlation between the activation energies for fluidities and molar conductivities of the 0.1 mol kg⁻¹ MX/PEO–H_2O systems. The broken line represents Eq. 12 with $p=0.89$ and the solid line represents the best-fit equation (13).

In contrast to the activation energy (enthalpy term), no significant correlation can be observed between the frequency factors (entropy term), A_Λ and A_ϕ, except in the case of PEG 200–H_2O systems (see Fig. 7).

A number of empirical entropy-enthalpy relationships have been known in the study of chemical reactions, both static and kinetic, in solution.[11,12] The

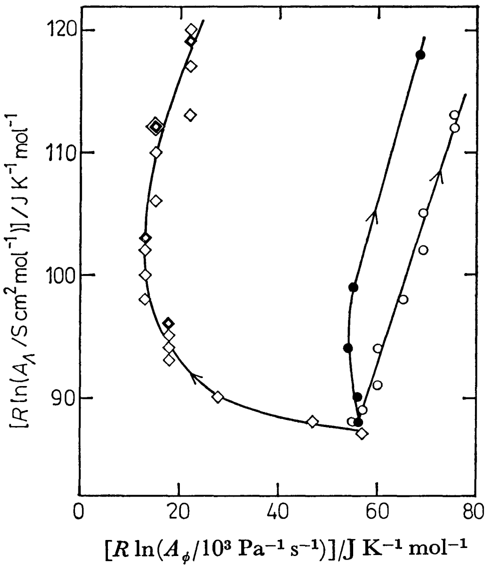

Fig. 7. Plots of $R \ln A_\Lambda$ against $R \ln A_\phi$ of the MX/PEO–H_2O systems: —○— PEG 200, —●— PEG 4000, and —◇— PEG 20000. Arrows indicate the direction of increasing PEO-concentration.

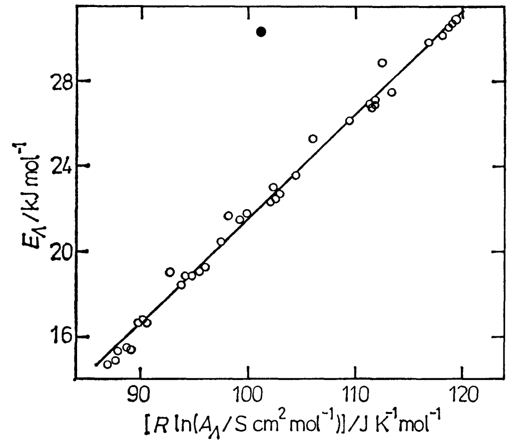

Fig. 8. Correlation between E_Λ and $R \ln A_\Lambda$ (isokinetic relationship) for the molar conductivities of MX in 0.1 mol kg^{-1} MX/PEO–H_2O systems. The solid circle corresponds to the NaCl/pure PEG 200 system, and the solid line represents the best-fit equation (14).

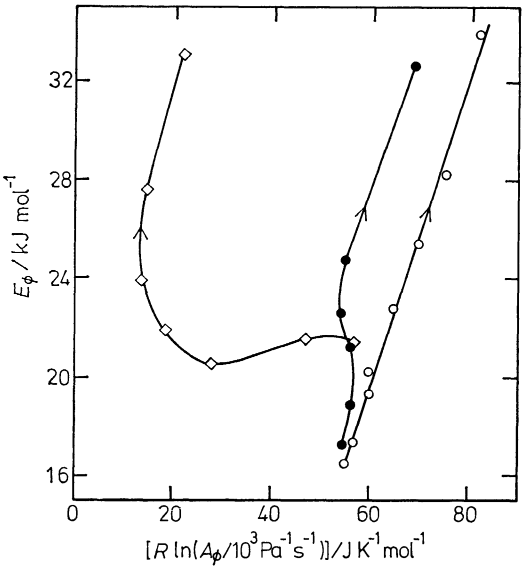

Fig. 9. Plots of E_ϕ against $R \ln A_\phi$ for the fluidity of PEO–H_2O mixtures: —○— PEG 200, —●— PEG 4000, and —◇— PEG 20000. Arrows indicate the direction of increasing PEO-concentration.

analysis of the activation parameters for the viscous flow and conductivity of the MX/PEO–H_2O systems has revealed a good correlation between E_Λ and $\ln A_\Lambda$, but no correlation between E_ϕ and $\ln A_\phi$, as is shown in Figs. 8 and 9. Except for the point corresponding to the NaCl/pure PEG 200 system, the analysis of 37 sets of data in Fig. 8 gives the following equation, representing the E_Λ *vs.* $R \ln A_\Lambda$ relationship:

$$E_\Lambda = T_c R \ln \frac{A_\Lambda}{\mathrm{S\ cm^2\ mol^{-1}}} - (27.5 \pm 0.74)\ \mathrm{kJ\ mol^{-1}} \quad (14)$$

with $T_c = 489.6 \pm 7.3$ K and the correlation coefficient $r = 0.9962$, and where T_c, the slope of the E_Λ *vs.* $R \ln A_\Lambda$ plot, is called the isokinetic or compensation temperature.[12] This relationship means that, in the case of the conductivity of the MX/PEO–H_2O system, the enthalpy of activation is partly compensated for by the entropic term (the enthalpy-entropy compensation effect) upon the variation in the composition of the system. Although the physical meaning of this correlation is not well known, the relation may be expected to originate in the solvent-solute interactions.[11,12] The significant deviation of the NaCl/pure PEG 200 system from the above-mentioned correlation suggests that the thermodynamic factors controlling the electric conduction will be different in pure PEO media from those in solutions containing water.

Conclusion. Our observations on the composition and temperature dependence of the fluidity and conductivity of the 0.1 mol kg^{-1} MX/PEO–H_2O systems can be summarized as follows: (1) The systems exhibited a linear relationship between $\ln A_{MX}$ and $\ln \phi$ (extended Walden's rule) upon the temperature variation at a constant composition, but not upon an isothermal variation in the PEO-concentration. (2) A good correlation was observed between the activation energies of the viscous flow and the conductivity, but not between the corresponding entropy terms (frequency factors). (3) The conductivity exhibited an enthalpy-entropy compensation effect (the isokinetic relationship) upon a variation in the composition of the system, while such a relationship could not be obtained in the case of the viscous flow.

When the PEO concentration increases at a constant temperature, the molar conductivity of 0.1 mol kg^{-1} MX in PEO–H_2O mixtures will decrease not only upon a lowering of the fluidity, but also by an increase in the ion association due to the decrease in the dielectric constant of the solution. The dielectric constants of PEO–H_2O mixtures have been reported to decrease almost linearly with an increase in the volume fraction of PEO, independent of the molar mass of PEO, in nearly the same way as in the case of dioxane–H_2O mixtures.[13] A rough estimation based on the knowledge concerning the ion-association constants for some alkali halides in dioxane–H_2O mixtures[14] shows that the degree of dissociation of 0.1 mol kg^{-1} MX in the PEO–H_2O mixtures will begin to decrease from unity at the mass fraction of PEO $w \simeq 0.4$ and reach about 0.3 at $w \simeq 0.6$. If the conductivity of the MX/PEO–H_2O system is corrected for the ion-association effect, the deviation from Walden's rule for the ionic mobilities of the ions should become greater than that observed for the molar conductivities. The above-mentioned consideration suggests that the ion-association effect cannot be ignored in discussing the conductivity of the MX/PEO–H_2O system. In this paper, however, no further consideration will be made of the ion-association effect because the present study is intended to examine some phenomenological relationships and not to make detailed mechanistic discussions.

It is suggested that the mechanisms controlling the viscous flow and electric conduction of the MX/PEO–H_2O system may be similar from the enthalpic standpoint, but may be significantly different from the entropic point of view. In the aqueous solutions of PEO, the long-chain polymer molecules will typically exist as random coils and will occasionally from a loosely coupled network. The Arrhenius-type expression (Eq. 5) shows that very low values of the macroscopic fluidity of the solutions containing large PEO molecules can be attributed to the decrease in the pre-exponential factor (entropy term), which is itself due to the formation of the very loose network structure consisting of the polymer chains and which cannot be compensated for by the enthalpy term. For small ions, however, there remain in the solution sufficiently large spaces to move around in, filled with water molecules in the normal condition, and the movement of the ions would not be appreciably disturbed by the low macroscopic fluidity. The correlations between pairs of the activation parameters observed in this study are consistent with the above-mentioned consideration of the ion-transport mechanism in the PEO–H_2O mixtures.

We wish to thank Dr. Yoshihiko Sugiura for the viscosity measurements using a rotational viscometer, and Dr. Haruo Honma for the determination of the relative molecular masses of the PEO samples.

References

1) For example: D. J. Jloyd, "The Problem of Gel Structure," in "Colloid Chemistry," ed by J. Alexander, The Chemical Catalog Company, New York (1926), Vol. I, pp. 775-776; P. H. Hermans, "Gels," in "Colloid Science," ed by H. R. Kruyt, Elsevier, Amsterdam (1949), Vol. II, Chap. XII; R. L. Kay, "Ionic Transport in Water and Mixed Aqueous Solvents," in "Water, A Comprehensive Treatise," ed by F. Franks, Plenum Press, New York (1973), Vol. 3, Chap. 4.

2) R. A. Robinson and R. H. Stokes, "Electrolyte Solutions," Butterworths, London (1965), Revised Ed., pp. 302—313.

3) J. M. Stokes and R. H. Stokes, *J. Phys. Chem.*, **62**, 497 (1958).

4) C. Treiner and R. M. Fuoss, *J. Phys. Chem.*, **69**, 2576 (1965).

5) R. H. Stokes and R. Mills, "Viscosity of Electrolytes and Related Properties," Pergamon, Oxford (1965), Chap. 6.

6) R. Tamamushi and K. Takahashi, *J. Electroanal. Chem.*, **50**, 277 (1974).

7) T. Isono, *Rikagaku Kenkyusho Hokoku*, **56**, 55 (1980).

8) R. H. Stokes and R. Mills, "Viscosity of Electrolytes and Related Properties," Pergamon, Oxford (1965), Chap. 7.

9) S. Glasstone, K. J. Laidler, and H. Eyring, "The Theory of Rate Processes," McGraw-Hill, New York (1941), Chaps. IX and X.

10) J. Jarzynski and C. M. Davis, "The Viscosity of Water," in "Water and Aqueous Solutions," ed by R. A. Horne, Wiley-Interscience, New York (1972), Chap. 17.

11) E. A. Moelwyn-Hughes, "Chemical Statics and Kinetics of Solutions," Academic Press, London (1971), Chap. 15.

12) J. B. F. N. Engberts, "Mixed Aqueous Solvent Effects on Kinetics and Mechanisms of Organic Reactions," in "Water, A Comprehensive Treatise," ed by F. Franks, Plenum Press, New York (1979), Chap. 4.

13) U. Kaatze, *Prog. Colloid Polym. Sci.*, **65**, 214 (1978).

14) J. E. Lind, Jr. and R. M. Fuoss, *J. Phys. Chem.*, **65**, 999 (1961); C. F. Mattina and R. M. Fuoss, *ibid.*, **79**, 1604 (1975).